MITSUBISHI ELECTRIC RESEARCH LABORATORIES
http://www.merl.com

Distributed secondary voltage controller for droop-controlled microgrids to improve power quality in power distribution networks

Wang, Z.; Sun, H.; Nikovski, D.N.

TR2016-096 July 2016

Abstract

A distributed secondary voltage controller is designed for droop-controlled microgrids in power distribution networks to improve power quality. Microgrids are typically managed by the droop control mechanism that ensures stability but does not guarantee power quality of voltage magnitude. To solve this power quality problem, the proposed distributed secondary voltage controller maintains a constant voltage at a microgrid's point of common coupling (PCC) using only local measurements. With the voltage regulation capability, a microgrid can be used to improve power quality so that greatly promote the microgrid's value to power system daily operations. The improved voltage regulation in a power network is demonstrated through simulation tests of a modified IEEE 37- node test feeder. Furthermore, this secondary voltage controller is compatible with existing voltage control devices, such as tapchanging transformers that automatically regulate voltage.

IEEE Power & Energy Society General Meeting

Distributed secondary voltage controller for droop-controlled microgrids to improve power quality in power distribution networks

Zhao Wang
Department of Electrical Engineering
University of Notre Dame
Notre Dame, IN 46556
Email: zwang6@nd.edu

Hongbo Sun and Daniel Nikovski
Mitsubishi Electric Research Laboratories
Cambridge, MA 02139
Email: hongbosun@merl.com, nikovski@merl.com

***Abstract*—A distributed secondary voltage controller is designed for droop-controlled microgrids in power distribution networks to improve power quality. Microgrids are typically managed by the droop control mechanism that ensures stability but does not guarantee power quality of voltage magnitude. To solve this power quality problem, the proposed distributed secondary voltage controller maintains a constant voltage at a microgrid's point of common coupling (PCC) using only local measurements. With the voltage regulation capability, a microgrid can be used to improve power quality so that greatly promote the microgrid's value to power system daily operations. The improved voltage regulation in a power network is demonstrated through simulation tests of a modified IEEE 37-node test feeder. Furthermore, this secondary voltage controller is compatible with existing voltage control devices, such as tap-changing transformers that automatically regulate voltage.**

***Index Terms*—Microgrid, droop control, secondary controller, voltage stability, ancillary service.**

I. Introduction

The microgrid concept is proposed to improve the power quality and reliability by providing power services locally [1] using intermittent renewable energy resources. A microgrid, however, is typically required to behave like a conventional load to minimize its impact on power distribution networks. To make microgrids play a more important role in a power system, a microgrid should improve the power quality at its point of common coupling (PCC) in terms of voltage magnitude. Maintaining power quality is a challenging task for droop-controlled microgrids. Although droop controllers help a microgrid to ensure stability, its power quality is usually not well maintained. For instance, the traditional reactive power-voltage (Q-E) droop controller leads to a voltage deviation proportional to its additional reactive power injection. Deviated voltage magnitudes make distribution system operators unable to predict the power quality of a microgrid hence reluctant to incorporate microgrids into their daily operations.

Recent research on droop-controlled microgrids did not solve this power quality problem. A consensus-based distributed voltage control method was proposed in [2] that solved the reactive power sharing among microgrids. Although the reactive power injection from each generation unit was specified, the power quality still degraded when power system parameters changed. A finite-time distributed voltage controller was proven to restore voltage magnitude for a droop-controlled microgrid [3]. However, both types of design required a frequent information exchange between neighboring controllers, which was unrealistic for a power distribution network coupled with geographically distributed microgrids. A quadratic voltage droop controller was proposed in [4][5] and proven to be exponentially stable [4][5][6]. However, voltage magnitudes still deviated from their nominal values when load levels changed, as demonstrated in their simulation results. As a result, these recent research efforts did not fully solve the power quality problem for droop-controlled microgrids in a power distribution network.

To solve this power quality problem, a distributed secondary voltage controller is proposed for the primary Q-E droop control widely used at a microgrid's PCC. This secondary voltage controller uses local information to determine a control input for the primary droop control. The additional control maintains a constant voltage at a microgrid's PCC regardless of load or state changes in the power distribution network. Even when the local load at the PCC constantly changes, the secondary voltage controller cancels the local load's impact on the voltage magnitude hence providing voltage regulation. Since a microgrid improves the power quality at its PCC, distribution system operators are more willing to integrate microgrids. Simulation test results show improved voltage regulation using the proposed secondary voltage controller over merely the primary Q-E droop controller or using the quadratic droop controller in [4][5]. In addition, the distributed secondary voltage controller is compatible with existing voltage control devices, therefore reduces the operation cost of a mirogrid-connected power distribution network.

The remainder of this paper is organized as follows. Section II introduces notations. Section III describes voltage control dynamics of the droop-controlled microgrid with key assumptions. Section IV introduces the distributed secondary voltage controller with voltage stability proof. Simulation results in Section V demonstrate improved power quality using the distributed secondary voltage controller. Section VI provides concluding remarks.

II. Notations

Three-phase balanced operation and per-unit (p.u.) normalization are basic assumptions. Under these assumptions, the admittance matrix $\boldsymbol{Y}_{n\times n}$ of an n-bus power network is defined as a complex matrix [7]. The shunt admittance at bus i is not included in $\boldsymbol{Y}_{n\times n}$, but considered as a shunt device in the load model. The admittance matrix $\boldsymbol{Y}_{n\times n}$ is also expressed

*This work was performed during Zhao Wang's internship at MERL.

as $\boldsymbol{G}_{n\times n} + j\boldsymbol{B}_{n\times n}$, where $\boldsymbol{G}_{n\times n}$ is the conductance matrix and $\boldsymbol{B}_{n\times n}$ is the susceptance matrix. Each component of the admittance matrix is expressed in either a rectangular form as $Y_{ij} = G_{ij} + jB_{ij}$ or a polar form as $Y_{ij} = |Y_{ij}|\angle\phi_{ij}$.

Each bus connects a generator and a load. $P_{gen,i}$ and $Q_{gen,i}$ denote generated power; $P_{load,i}$ and $Q_{load,i}$ are real and reactive loads. At any bus i, E_i is the voltage magnitude and δ_i is the phase angle; P_i and Q_i are injected power; $\theta_{ij} = \delta_i - \delta_j$ is the phase angle difference between bus i and j. Power injections at bus i are $P_i = P_{gen,i} - P_{load,i}$ and $Q_i = Q_{gen,i} - Q_{load,i}$. With no power generation whatsoever, a pure load bus j has $P_j + P_{load,j} = 0$ and $Q_j + Q_{load,j} = 0$.

Using these state definitions, power injections P_i and Q_i at any bus i are expressed in the *power flow* relationship as

$$P_i = \sum_{j=1,j\neq i}^{n} |Y_{ij}| \left[E_i E_j \cos(\theta_{ij} - \phi_{ij}) - E_i^2 \cos\phi_{ij}\right], \quad (1)$$

$$Q_i = \sum_{j=1,j\neq i}^{n} |Y_{ij}| \left[E_i^2 \sin\phi_{ij} + E_i E_j \sin(\theta_{ij} - \phi_{ij})\right], \quad (2)$$

Parameters $|Y_{ij}|$ and ϕ_{ij} are initially determined by power network planning then constantly vary due to protection and control actions. Although possible in a power transmission system, keeping the updated knowledge of the entire power distribution network is not realistic.

Based on the power flow relationship above, a set point is defined as $(\boldsymbol{E}_{set}, \boldsymbol{\theta}_{set}, \boldsymbol{P}_{set}, \boldsymbol{Q}_{set}, \omega_{set})$, where ω_{set} is generally the nominal angular frequency ω_0. The set point is usually the solution to an optimal power flow (OPF) problem. As system parameters change during operations, states deviate from the set point and the error states at bus i are defined as $\tilde{E}_i = E_i - E_{set,i}$, $\tilde{P}_i = P_{set,i} - P_i$, $\tilde{Q}_i = Q_{set,i} - Q_i$.

A power network, or a microgrid, includes various types of loads that are represented in a ZIP load model [8] combining constant-impedance (Z), constant-current (I) and constant-power (P) components. Real and reactive loads at any bus i are defined as functions of voltage magnitude E_i (in p.u.) as

$$P_{load,i} = E_i^2 P_{Z-load,i} + E_i P_{I-load,i} + P_{P-load,i}, \quad (3)$$

$$Q_{load,i} = E_i^2 Q_{Z-load,i} + E_i Q_{I-load,i} + Q_{P-load,i}, \quad (4)$$

where $P_{Z-load,i}$ and $Q_{Z-load,i}$ are nominal constant-impedance loads, including shunt devices; $P_{I-load,i}$ and $Q_{I-load,i}$ are nominal constant-current loads, denoting devices that are modeled as current sources; $P_{P-load,i}$ and $Q_{P-load,i}$ are nominal constant-power loads, generally as a result of some power control mechanism.

The nominal load values $P_{load,set,i}$ and $Q_{load,set,i}$ are expressed as $P_{load,set,i} = E_i^2 P_{Z-load,set,i} + E_i P_{I-load,set,i} + P_{P-load,set,i}$ and $Q_{load,set,i} = E_i^2 Q_{Z-load,set,i} + E_i Q_{I-load,set,i} + Q_{P-load,set,i}$. Combining the load expressions above, load changes $\Delta P_{load,i} = P_{load,i} - P_{load,set,i}$ and $\Delta Q_{load,i} = Q_{load,i} - Q_{load,set,i}$ are defined as

$$\Delta P_{load,i} = E_i^2 \Delta P_{Z-load,i} + E_i \Delta P_{I-load,i} + \Delta P_{P-load,i},$$
$$\Delta Q_{load,i} = E_i^2 \Delta Q_{Z-load,i} + E_i \Delta Q_{I-load,i} + \Delta Q_{P-load,i}.$$

$\Delta P_{Z-load,i}$ and $\Delta Q_{Z-load,i}$ are changes of the constant-impedance component; $\Delta P_{I-load,i}$ and $\Delta Q_{I-load,i}$ are changes of the constant-current component; $\Delta P_{P-load,i}$ and $\Delta Q_{P-load,i}$ are changes of the constant-power component.

III. System Model

An n-bus power distribution network is modeled with m microgrids and l pure load buses, so that there is $n = m + l$. *Assumption* 1 is important because it leads to a simple and accurate power flow expression at a microgrid's PCC.

Assumption 1: The microgrid at bus i connects to the power distribution network through its PCC to a pure load bus j.

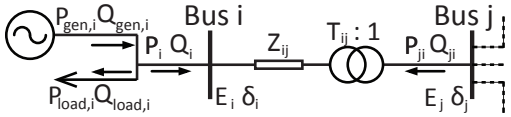

Fig. 1. A general branch model of the connection link between bus i and j.

In Figure 1, a general branch model represents either a transmission line or a transformer with a tap changer. T_{ij} is the tap value. Specifically, the tap value of a transmission line is $T_{ij} = 1$. With a little abuse of notation, Y_{ij} is defined as $Y_{ij} = -\frac{1}{Z_{ij}}$, where Z_{ij} is the connection link's impedance.The power flow expression transforms to

$$P_i = |Y_{ij}| \left[T_{ij} E_i E_j \cos(\theta_{ij} - \phi_{ij}) - E_i^2 \cos\phi_{ij}\right], \quad (5)$$

$$Q_i = |Y_{ij}| \left[E_i^2 \sin\phi_{ij} + T_{ij} E_i E_j \sin(\theta_{ij} - \phi_{ij})\right]. \quad (6)$$

The real and reactive power flows from bus j to bus i are

$$P_{ji} = |Y_{ij}| \left[T_{ij} E_i E_j \cos(\theta_{ij} + \phi_{ij}) - T_{ij}^2 E_j^2 \cos\phi_{ij}\right],$$
$$Q_{ji} = |Y_{ij}| \left[T_{ij}^2 E_j^2 \sin\phi_{ij} - T_{ij} E_i E_j \sin(\theta_{ij} + \phi_{ij})\right].$$

Using the expression of Q_i in equation (6), the reactive power error $\tilde{Q}_i$ is a function of the voltage error $\tilde{E}_i$, as follows

$$\begin{aligned}\tilde{Q}_i = &-(2E_{set,i}\tilde{E}_i + \tilde{E}_i^2)|Y_{ij}|\sin\phi_{ij} \\ &-T_{ij}\tilde{E}_i E_j |Y_{ij}|\sin(\theta_{ij} - \phi_{ij}) \\ &-T_{ij} E_{set,i} E_j |Y_{ij}|\sin(\theta_{ij} - \phi_{ij}) \\ &+T_{set,ij} E_{set,i} E_{set,j} |Y_{ij}|\sin(\theta_{set,ij} - \phi_{ij}), \\ = &-\tilde{E}_i^2 |Y_{ij}|\sin\phi_{ij} - T_{ij} E_{set,i} E_j |Y_{ij}|\sin(\theta_{ij} - \phi_{ij}) \\ &-\tilde{E}_i [2E_{set,i}|Y_{ij}|\sin\phi_{ij} + T_{ij} E_j |Y_{ij}|\sin(\theta_{ij} - \phi_{ij})] \\ &+T_{set,ij} E_{set,i} E_{set,j} |Y_{ij}|\sin(\theta_{set,ij} - \phi_{ij}),\end{aligned} \quad (7)$$

where $T_{set,ij}$ is the nominal tap value at the set point. Similarly, the load variation is also a function of $\tilde{E}_i$ as

$$\begin{aligned}&Q_{load,set,i}(E_{set,i}) - Q_{load,i}(E_i) \\ &= -(2E_{set,i}\tilde{E}_i + \tilde{E}_i^2) Q_{Z-load,set,i} - Q_{I-load,set,i}\tilde{E}_i \\ &\quad -(E_i^2 \Delta Q_{Z-load,i} + E_i \Delta Q_{I-load,i} + \Delta Q_{P-load,i}), \\ &= -\tilde{E}_i^2 Q_{Z-load,set,i} - \Delta Q_{load,i}(E_i) \\ &\quad -\tilde{E}_i (2E_{set,i} Q_{Z-load,set,i} + Q_{I-load,set,i}).\end{aligned} \quad (8)$$

As shown in Figure 2, a Q-E droop controller manages the voltage magnitude at a microgrid's PCC with dynamics

$$\dot{E}_i = (E_{ref,i} - E_i) - m_{Q,i} Q_{gen,i}, \quad (9)$$

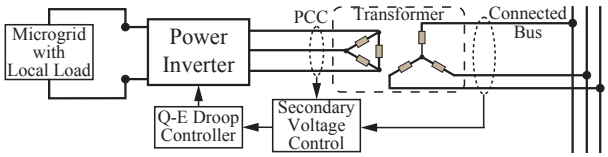

Fig. 2. The secondary voltage controller is implemented at a microgrid's PCC using measurements on both sides of the step-up transformer.

where $m_{Q,i}$ is the droop slope of the Q-E droop controller; $E_{ref,i}$ is the voltage control command; $Q_{gen,i}$ is the reactive power generation from the microgrid. At steady state, the injected reactive power from the microgrid is proportional to the voltage difference between $E_{ref,i}$ and E_i. The additional reactive power injection prevents the voltage magnitude E_i changing further so that stabilizes voltage. The control command $E_{ref,i}$, designated by a distribution system operator, is determined based on the set point $(\boldsymbol{E}_{set}, \boldsymbol{\theta}_{set}, \boldsymbol{P}_{set}, \boldsymbol{Q}_{set}, \omega_{set})$ as

$$E_{ref,i} = E_{set,i} + m_{Q,i}(Q_{set,i} + Q_{load,set,i}(E_{set,i})). \quad (10)$$

For comparison purposes, a quadratic voltage droop controller [4] is also considered, whose dynamic equation is

$$\dot{E}_i = \frac{E_i}{E_{set,i}}(E_{ref,i} - E_i) - m_{Q,i}Q_{gen,i}. \quad (11)$$

The voltage feedback signal is scaled by a ratio of E_i over the set point $E_{set,i}$. Although exponential voltage stability was proven, the voltage magnitude at each microgrid's PCC still deviates when network parameters changed.

IV. Main Result

A distributed secondary voltage controller is introduced that maintains a constant voltage magnitude at a microgrid's PCC regardless of changes in the power distribution network. Exponential voltage stability is then proven with a bound of converging speed over the region of attraction. Furthermore, input-output stability is established when disturbances, such as measurement error, are considered in the proposed controller.

A. Secondary Voltage Controller

The distributed secondary voltage controller adds a control input u_i to the Q-E droop controller in equation (9) as

$$\dot{E}_i = (E_{ref,i} - E_i) - m_{Q,i}Q_{gen,i} + m_{Q,i}u_i. \quad (12)$$

This control input is designed as

$$u_i = (Q_i - Q_{set,i}) - (E_i^2 - E_{set,i}^2)B_{ij} + \Delta Q_{load,i}, \quad (13)$$

which uses local information available at a microgrid's PCC, such as Q_i, E_i and $\Delta Q_{load,i}$. Using this secondary voltage controller for a droop-controlled microgrid, asymptotic voltage stability is established in the following theorem.

Theorem 1: For a droop-controlled microgrid at bus i with the control input in equation (13), the voltage E_i at bus i asymptotically converges to the set point $E_{set,i}$ if $b_i > 0$

$$\begin{cases} E_i > -\frac{b_i}{a_i} + E_{set,i}, & \text{when } a_i > 0, \\ E_i < -\frac{b_i}{a_i} + E_{set,i}, & \text{when } a_i < 0. \end{cases}$$

where $a_i = Q_{Z-load,set,i} + B_{ij}$ and $b_i = \frac{1}{m_{Q,i}} + Q_{I-load,set,i} + 2E_{set,i}(Q_{Z-load,set,i} + B_{ij})$.

Proof: Based on voltage control dynamics in equation (12) and $E_{ref,i}$ expression, the voltage error dynamics are

$$\begin{aligned} \dot{\tilde{E}}_i &= (E_{set,i} - E_i) + m_{Q,i}(Q_{set,i} - Q_i) \\ &\quad + m_{Q,i}(Q_{load,set,i}(E_{set,i}) - Q_{load,i}(E_i)) + m_{Q,i}u_i, \\ &= -\tilde{E}_i + m_{Q,i}\tilde{Q}_i + m_{Q,i}u_i \\ &\quad + m_{Q,i}(Q_{load,set,i}(E_{set,i}) - Q_{load,i}(E_i)). \end{aligned}$$

The control input in equation (13) is rewritten as a polynomial

$$\begin{aligned} u_i &= (Q_i - E_i^2 B_{ij}) - (Q_{set,i} - E_{set,i}^2 B_{ij}) + \Delta Q_{load,i}(E_i), \\ &= T_{ij}E_iE_j|Y_{ij}|\sin(\theta_{ij} - \phi_{ij}) + \Delta Q_{load,i}(E_i) \\ &\quad - T_{set,ij}E_{set,i}E_{set,j}|Y_{ij}|\sin(\theta_{set,ij} - \phi_{ij}), \\ &= T_{ij}\tilde{E}_iE_j|Y_{ij}|\sin(\theta_{ij} - \phi_{ij}) + \Delta Q_{load,i}(E_i) \\ &\quad + T_{ij}E_{set,i}E_j|Y_{ij}|\sin(\theta_{ij} - \phi_{ij}) \\ &\quad - T_{set,ij}E_{set,i}E_{set,j}|Y_{ij}|\sin(\theta_{set,ij} - \phi_{ij}), \\ &= -u_{a,i}\tilde{E}_i^2 - u_{b,i}\tilde{E}_i - u_{c,i}, \end{aligned}$$

where $u_{a,i} = 0$, $u_{b,i} = -T_{ij}E_j|Y_{ij}|\sin(\theta_{ij} - \phi_{ij})$, and $u_{c,i} = T_{set,ij}E_{set,i}E_{set,j}|Y_{ij}|\sin(\theta_{set,ij} - \phi_{ij}) - T_{ij}E_{set,i}E_j|Y_{ij}|\sin(\theta_{ij} - \phi_{ij}) - \Delta Q_{load,i}(E_i)$. Combined with expressions in equation (7) and (8), dynamics of $\tilde{E}_i$ is

$$\dot{\tilde{E}}_i = -m_{Q,i}(a_i\tilde{E}_i^2 + b_i\tilde{E}_i),$$

whose equilibrium point is $\tilde{E}_i = 0$, i.e. $E_i = E_{set,i}$. With respect to this equilibrium point, a candidate local Lyapunov function is defined as $V_i = \frac{1}{2m_{Q,i}}\tilde{E}_i^2$ whose derivative is

$$\dot{V}_i = \tilde{E}_i(-a_i\tilde{E}_i^2 - b_i\tilde{E}_i) = -(a_i\tilde{E}_i + b_i)\tilde{E}_i^2.$$

As long as $a_i\tilde{E}_i + b_i > 0$ at bus i, the voltage magnitude E_i asymptotically converges to the set point $E_{set,i}$. When $a_i > 0$ and $b_i > 0$, there is $\tilde{E}_i > -\frac{b_i}{a_i}$, i.e. $E_i > -\frac{b_i}{a_i} + E_{set,i}$; when $a_i < 0$ and $b_i > 0$, there is $\tilde{E}_i < -\frac{b_i}{a_i}$, i.e. $E_i < -\frac{b_i}{a_i} + E_{set,i}$. ■

Remark 1: Between a distribution system operator's updates of voltage control command $E_{ref,i}$, the secondary voltage controller maintains a constant voltage at a microgrid's PCC regardless of changes in the power distribution network.

Remark 2: The parameter B_{ij} in the input u_i is determined in real-time based on measurements available at bus i.

B. Exponential Stability and Input-Output Stability

Besides asymptotic stability, the secondary voltage controller leads to exponential stability with respect to the set point $E_{set,i}$ at a guaranteed converging speed. The following theorem proves exponential stability of voltage E_i at bus i.

Theorem 2: Using the control input in equation (13), voltage E_i is exponentially stable with respect to $E_{set,i}$ over

$$\left[-\frac{\frac{1}{m_{Q,i}} + Q_{I-load,set,i}}{2|a_i|}, 2E_{set,i} + \frac{\frac{1}{m_{Q,i}} + Q_{I-load,set,i}}{2|a_i|}\right],$$

whose converging speed is faster than $\dot{\tilde{E}}_i = -\frac{m_{Q,i}}{2}b_i\tilde{E}_i$.

Proof: The set point $E_i = E_{set,i}$ (or $\tilde{E}_i = 0$) is an isolated equilibrium point over $E_i \in [0, +\infty)$. Over a smaller range, the converging speed of the voltage error $\tilde{E}_i$ is bounded by a first-order dynamic system. When $a_i > 0$, there is $\dot{\tilde{E}}_i \geq -\frac{b_i}{2} m_{Q,i} \tilde{E}_i \geq 0$ over the range $\tilde{E}_i \in (-\frac{b_i}{a_i}, +\infty)$; when $a_i < 0$, there is $\dot{\tilde{E}}_i \leq -\frac{b_i}{2} m_{Q,i} \tilde{E}_i \leq 0$ over the range $\tilde{E}_i \in (-\infty, -\frac{b_i}{a_i})$. A special case is when $a_i = 0$, where the voltage error range is $(-\infty, +\infty)$ and the dynamic equation is simply $\dot{\tilde{E}}_i = -b_i m_{Q,i} \tilde{E}_i$. Obviously, the converging speed of $\tilde{E}_i$ is always faster than $\dot{\tilde{E}}_i = -\frac{b_i}{2} m_{Q,i} \tilde{E}_i$.

Combining all voltage error ranges above leads to $\tilde{E}_i \in \left[-\frac{b_i}{2|a_i|}, \frac{b_i}{2|a_i|}\right]$, where $\frac{b_i}{2|a_i|} = E_{set,i} + \frac{1/m_{Q,i} + Q_{I-load,set,i}}{2|a_i|}$. As a result, the range of voltage magnitude E_i is

$$\left[-\frac{\frac{1}{m_{Q,i}} + Q_{I-load,set,i}}{2|a_i|}, 2E_{set,i} + \frac{\frac{1}{m_{Q,i}} + Q_{I-load,set,i}}{2|a_i|}\right],$$

over which the Lyapunov function $V_i = \frac{\tilde{E}_i^2}{2m_{Q,i}}$ is bounded as

$$k_1 \tilde{E}_i^2 \leq V_i \leq k_2 \tilde{E}_i^2, \tag{14}$$

where $k_1 = k_2 = \frac{1}{2m_{Q,i}}$. The derivative of V_i to time is

$$\dot{V}_i = -(a_i \tilde{E}_i + b_i)\tilde{E}_i^2 \leq -\frac{b_i}{2} m_{Q,i} \tilde{E}_i^2 = -k_3 \tilde{E}_i^2, \tag{15}$$

where $k_3 = \frac{b_i}{2} m_{Q,i}$. Based on theorem 4.10 in [9], equilibrium point $E_i = E_{set,i}$ is exponentially stable over the domain. ■

The secondary voltage controller cancels the impact of local load variations using $\Delta Q_{load,i}(E_i)$ in the control input u_i, which is a function of local measurement and the nominal load values. If the measurements come with disturbance, such as measurement noise, there is a voltage magnitude error at the microgrid's PCC. According to theorem 5.1 in [9], small-signal input-output stability can be established for the proposed distributed secondary voltage controller.

V. Simulation Tests

The proposed distributed secondary voltage controller is examined in a modified IEEE 37-node test feeder [10], as shown in Figure 3. Besides microgrids and step-up transformers, all load buses are modified from unbalanced loads in the original model [11] to balanced ones by combining three-phase load values. Considering the power quality of voltage magnitude, simulation results demonstrate advantage of the distributed secondary voltage controller over the traditional droop control and the quadratic droop control [4][5]. Besides improved power quality, the secondary voltage controller is also compatibility with existing voltage-control mechanisms and reduces the operation cost by switching less frequently.

In Figure 3, three microgrids connect to the power distribution network through transformers that automatically regulate the voltage at each microgrid's PCC. There are nine taps (between 0.95p.u. and 1.05p.u.) at the low-voltage (microgrid) side of each transformer. Each tap change corresponds to a 0.0125p.u. (or 1.25%) of voltage magnitude variation with a mechanical delay of 4.0 seconds. The dead band of voltage regulation is between 0.9875 p.u. and 1.0125 p.u.. Besides the information exchanged between two sides of each transformer, there is *NO* global communication, which is the situation in a power distribution network. Pure load buses have constant-power load, with fixed real and reactive power consumption, as defined in [10]. The load at each pure load bus has a normally distributed noise whose standard deviation is 2.5% of its nominal value. The power distribution network in Figure 3 operates at 60Hz and has a base power of 100kVA. Each microgrid's PCC is managed by droop control mechanism whose parameters are shown in Table I. M is the inertia and D is the damping ratio. $\underline{P}_{gen,i}$ and $\overline{P}_{gen,i}$ are lower and upper real-power generation limits. $\underline{Q}_{gen,i}$ and $\overline{Q}_{gen,i}$ are lower and upper reactive-power generation limits.

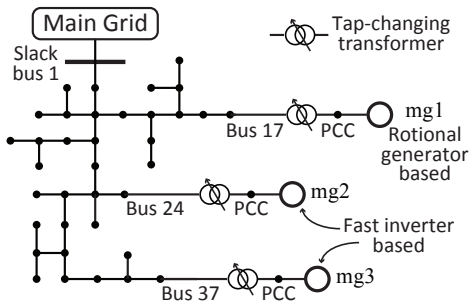

Fig. 3. The modified IEEE 37-node feeder operates at 60Hz with 100kVA base power with three microgrids connected through transformers.

TABLE I
Droop controller parameter at each microgrid's PCC

#	m_Q p.u.	M $\frac{p.u.}{(\frac{rad}{s})^2}$	D $\frac{p.u.}{\frac{rad}{s}}$	ω_0 $\frac{rad}{s}$	$\frac{\underline{P}_{gen,i}}{\overline{P}_{gen,i}}$	$\frac{\underline{Q}_{gen,i}}{\overline{Q}_{gen,i}}$
1	0.25	0.0507	0.1959	120π	$[0.6, 1.37]$	$[-3.0, 3.0]$
2	0.167	0.0032	0.3138	120π	$[1.0, 2.0]$	$[-4.0, 4.0]$
3	0.25	0.0023	0.2315	120π	$[0.7, 1.4]$	$[-3.0, 3.0]$

The simulation results are shown in Figure 4 and Figure 5. In each simulation, the load at a microgrid's PCC increases to a peak value between $t = 5$sec and 25sec, stays constant for five seconds and recovers to its original value in a linear fashion between $t = 30$sec and 50sec. The load variation over twenty seconds is slow enough such that no transient exists.

There is a 0.2 p.u. constant-power load increase at the PCC of microgrid 1 (mg1) in Figure 3, which has a major component of reactive power with a power factor of 0.2. As shown in Figure 4, the voltage magnitude of each microgrid's PCC keeps 1.0 p.u. when the local load changes so that the power quality within each microgrid is guaranteed. In addition, the proposed secondary voltage controller results in almost a constant voltage at pure load buses so that power quality improves throughout the entire power system. The microgrid's voltage set point is within the tap-changing transformer's dead band, so that the proposed secondary voltage controller is compatible with existing voltage control devices. Since it is unnecessary to change tap, as shown in Figure 5, tap changes

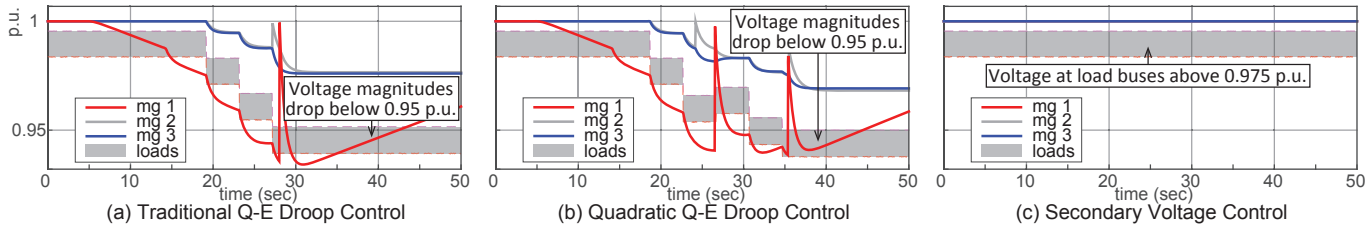

Fig. 4. Comparison of voltage magnitudes at each microgrid's PCC and load buses: (a) the traditional Q-E droop control causes voltage drop below 0.95p.u.; (b) the quadratic Q-E droop control leads to voltage drop below 0.95p.u.; (c) the secondary voltage control keeps the microgrid's PCC voltage at 1.0p.u..

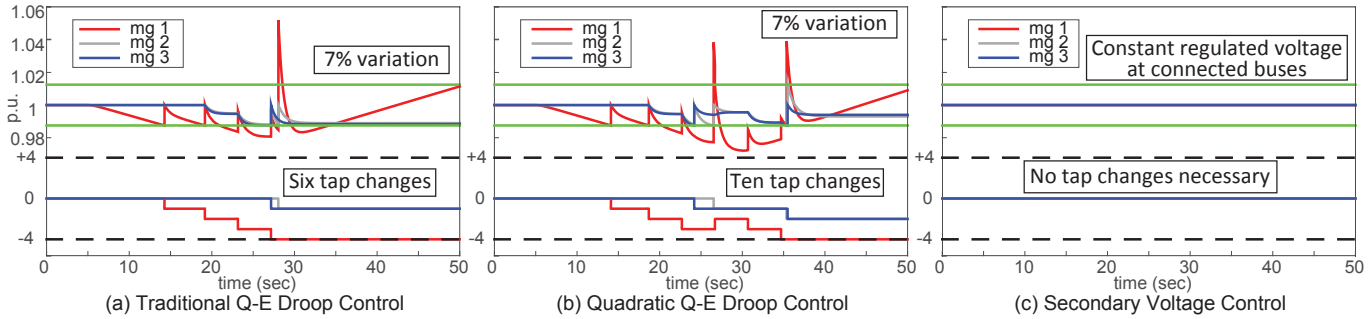

Fig. 5. Comparison of regulated voltages at connected bus 17, bus 24 and bus 37: (a) the traditional Q-E droop control leads to 7% variation; (b) the quadratic Q-E droop control causes 7% variation; (c) the secondary voltage control keeps a constant voltage at 1.0p.u. with no tap change necessary.

are less frequent hence reducing the operation cost.

Simulation results show improved power quality using the distributed secondary voltage controller over merely the primary Q-E droop controller or the quadratic droop controller in [4]. In addition, the distributed secondary voltage controller is compatible with existing voltage control devices, such as a transformer with a tap changer.

VI. Conclusion

A distributed secondary voltage controller is proposed to improve the power quality at a droop-controlled microgrid's PCC. Using local measurements, this secondary voltage controller maintains constant voltage magnitude at the microgrid's PCC with proven exponential stability. With voltage regulation capability, a microgrid improves power quality in power distribution networks so that greatly promotes a microgrid's value in power system daily operations. Simulation results not only show improved power quality in a power distribution network, but also demonstrate the distributed secondary voltage controller's compatibility with existing voltage control devices.

References

[1] R. Lasseter, "Smart distribution: Coupled microgrids," *Proceedings of the IEEE*, vol. 99, no. 6, pp. 1074–1082, 2011.

[2] J. Schiffer, T. Seel, J. Raisch, and T. Sezi, "A consensus-based distributed voltage control for reactive power sharing in microgrids," in *Control Conference (ECC), 2014 European*. IEEE, 2014, pp. 1299–1305.

[3] F. Guo, C. Wen, J. Mao, and Y.-D. Song, "Distributed secondary voltage and frequency restoration control of droop-controlled inverter-based microgrids," *Industrial Electronics, IEEE Transactions on*, vol. 62, no. 7, pp. 4355–4364, 2015.

[4] J. W. Simpson-Porco, F. Dorfler, and F. Bullo, "Voltage stabilization in microgrids using quadratic droop control," in *IEEE Conf. on Decision and Control, Florence, Italy*, 2013.

[5] J. W. Simpson-Porco, F. Dorfler, F. Bullo, Q. Shafiee, and J. M. Guerrero, "Stability, power sharing, & distributed secondary control in droop-controlled microgrids," in *Smart Grid Communications (SmartGridComm), 2013 IEEE International Conference on*. IEEE, 2013, pp. 672–677.

[6] B. Gentile, J. W. Simpson-Porco, F. Dorfler, S. Zampieri, and F. Bullo, "On reactive power flow and voltage stability in microgrids," in *American Control Conference (ACC), 2014*. IEEE, 2014, pp. 759–764.

[7] A. R. Bergen, *Power Systems Analysis, 2/E*. Pearson Education, 2009.

[8] "Load representation for dynamic performance analysis," *Power Systems, IEEE Transactions on*, vol. 8, no. 2, pp. 472–482, 1993.

[9] H. K. Khalil, *Nonlinear systems*. Prentice hall Upper Saddle River, 2002, vol. 3.

[10] (2010) Distribution test feeders. [Online]. Available: http://ewh.ieee.org/soc/pes/dsacom/testfeeders/

[11] W. H. Kersting, "Radial distribution test feeders," in *Power Engineering Society Winter Meeting, 2001. IEEE*, vol. 2. IEEE, 2001, pp. 908–912.

Appendix

Parameters of the link between bus i and bus j, i.e. $|Y_{ij}|$, ϕ_{ij} and T_{ij}, are determined to compute the secondary voltage control input. Available measurements include: real and reactive power injections at bus i, i.e. P_i and Q_i; real and reactive power flow from bus j to bus i, i.e. P_{ji} and Q_{ji}; voltage magnitudes at bus i and j, i.e. E_i and E_j.

For a tap-changing transformer that automatically regulates voltage, parameters ϕ_{ij}, $|Y_{ij}|$, and T_{ij} are determined as

$$\tan\phi_{ij} = \frac{Q_{ji}+Q_i}{-P_{ji}-P_i}, \quad \tan(\delta_i-\delta_j) = \frac{a_{T,i}}{\frac{P_i^2+Q_i^2}{b_{T,i}+c_{T,i}} - c_{T,i}},$$

$$|Y_{ij}| = \frac{c_{T,i}+\frac{a_{T,i}}{\tan(\delta_i-\delta_j)}}{E_i^2}, \text{ and } T_{ij} = \frac{a_{T,i}}{|Y_{ij}|E_iE_j\sin(\delta_i-\delta_j)},$$

where $a_{T,i} = P_i\sin\phi_{ij} + Q_i\cos\phi_{ij} = -P_{ji}\sin\phi_{ij} - Q_{ji}\cos\phi_{ij}$, $b_{T,i} = Q_{ji}\sin\phi_{ij} - P_{ji}\cos\phi_{ij}$, and $c_{T,i} = Q_i\sin\phi_{ij} - P_i\cos\phi_{ij}$.